35th Annual International Conference of the IEEE EMBS
Osaka, Japan, 3 - 7 July, 2013

Fusion of Lung MR/CT Images Through Lung Vessel Registration*

Yuma Iwao[1], Yingying Wei[1], Seiichiro Kagei[1], Toshiyuki Gotoh[1],
Tae Iwasawa[2] and Marcos de Sales Guerra Tsuzuki[3]

***Abstract*— Lung perfusion analysis with sequential contrasted MRI is an important clinical tool. This work is part of larger research in which the objective of fusing lung perfusion analysis and lung anatomical structures. In this work, it is proposed a multimodality MR/CT lung fusion algorithm based on lung vessel determination that analyzes lung perfusion. 3D contrasted MR and 3D CT images are first normalized (slice thickness, resolution and pixel intensity), then lung features are determined and elastically registered. The registration algorithm was checked by mapping in both directions, from MR to CT and vice-versa. A MR perfusion analysis result is fused with a 3D CT segmented lung vessel tree.**

I. Introduction

Registration techniques have been developed to improve the correlation between anatomical and physiological information obtained from different imaging modalities (SPECT, PET, CT and others) [1]. The clinical relevance of lung registration is underlined by the huge number of recent publications dealing with the topic. Gotoh et al. [2] proposed a lung registration algorithm for MRIs. Murphy et al. [3] surveyed several lung registration algorithms for CT images. However, the large non-linear deformations suffered by the lung within different inflation levels, makes the exact lung registration challenging, and advanced algorithms are required [1].

Lung perfusion analysis using sequential contrasted MRI has been widely researched, and it is turning to be a very important clinical tool [1]. The fusion of perfusion analysis and lung anatomical structures is a current topic of research in medical imaging. This work is a first step towards such fusion technique.

This paper is structured as follows. In section II, a lung vessel segmentation from CT images is presented. In section III, the proposed method of blood flow determination within 3D sequence of contrasted MRI is explained. Section IV presents the proposed MR/CT fusion algorithm. Section V presents a result where the perfusion information (from MR chest image) is fused with the segmented lung vessel (explained in section II), and section VI presents the conclusions.

*This project was partially supported by a JSPS KAKENHI Grant (24500539) and a joint project from JSPS/CAPES. [1]Y. Iwao, Y. Wei, S. Kagei and T. Gotoh are with Yokohama National University, 79-1 Tokiwadai, Hodogaya-ku, Yokohama-shi, Kanagawa, 240-8501, Japan. iwao-yuma-xg@ynu.jp, {kagei,gotoh}@ynu.ac.jp. [2]T. Iwasawa is with Kanagawa Cardiovascular Respiratory Center, Kanazawa–ku, Yokohama-shi, Kanagawa, 236-0051, Japan. tae_I_md@wb3.so-net.ne.jp. [3]M.S.G. Tsuzuki is with Escola Politécnica da Universidade de São Paulo, Brazil. Computational Geometry Laboratory. mtsuzuki@usp.br. This author was partially supported by CNPq.

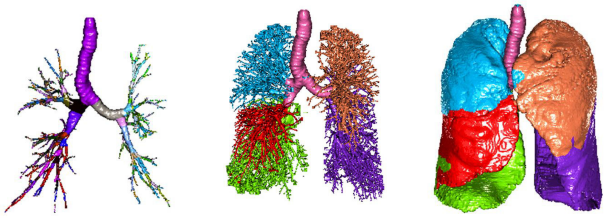

(a) (b) (c)

Fig. 1. Lung anatomical structures determined from a patient with IIPs. (a) Segmented airways. (b) Lung vessels segmentation. (c) Lung classified in lobes.

II. Lung Vessel Segmentation from CT Images

3D region growing algorithms are widely used for airway segmentation from CT images [4]. Region growing methods have a current pixel, and recursively search for similar adjacent pixels. The algorithm is simple and can be implemented with very high speed. On the other hand, such an algorithm can be easily influenced by noise, and it is not simple to segment bronchial trees with similar CT region intensities. The lung parenchyma periphery is a challenging region. Particularly, some situations that often happens can make the segmentation a hard problem: the lung parenchyma and intrabronchial regions can have their volumes partially filled with air; and diseases can produce wall thickness and unclear noise. To solve these problems, several algorithms have been proposed, mainly using specific rules [5].

The lungs are composed by five lobes: two in the left and three in the right. Inside each lobe, two structures exist without intersection: lung bronchial and vessel trees. The lung bronchial tree is mainly filled with air and the lung vessels are mainly filled with blood which has similar properties to water. Iwao et al. [6] proposed a region growing algorithm with failure tracking and recovery features that extracts lung airways and vessels (see Fig. 1.(a)-(b)). The determined lung airways and vessels are classified into five lobe regions. A Voronoi diagram is constructed using the bronchial and vessel trees. The lung lobes are determined using the Voronoi classification (see Fig. 1.(c)).

III. MR 3D Temporal Images with Contrast

After injecting a contrast into the blood, its passage through the vascular system can be monitored by 3D temporal MRI. It is assumed that there is no recirculation and that the patient is in breath hold with no movements, consequently it is expected to exhibit just a single peak in time. For each pixel, its maximum intensity in time is

978-1-4577-0216-7/13/$26.00 ©2013 IEEE

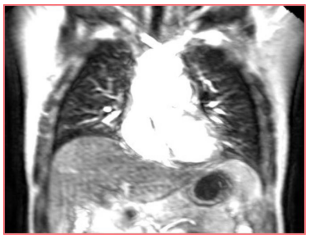

Fig. 2. MRI with each pixel with its maximum intensity in time.

determined (see Fig. 2). Such image is called as MR-MIT (MR with Maximum Intensity in Time).

IV. The Proposed Algorithm for MR/CT Fusion

MR and CT images have different characteristics (visible features, slice thickness and resolution, just enumerating a few). Additionally, both images were taken with the lung in distinct breathing state. The registration between CT and MR images is very challenging.

The proposed MR/CT fusion algorithm is shown in Fig. 3. The input are the two 3D images: CT and temporal contrasted MR. The proposed algorithm consists in two great steps in which are shown in the internal rectangle. The first step normalizes CT and MR features with the objective of creating a pixel by pixel direct mapping between them (slice thickness, resolution and pixel intensity). The second step searches for image features and creates a flexible registration among the determined image features. The fusion algorithm creates a mapping that can fuse the perfusion information with the segmented lung vessels (explained in section II).

A. MR and CT images Normalization

The first module in the first step, shown in Fig. 3, is the slice correspondence determination. The slice thickness for MR and CT are respectively 12 mm and 1 mm [1]. Both images, MR and CT, are processed to reduce their differences. Initially, adjacent CT images are grouped to have a correspondence with one MRI. The pixels with the same (x, y) coordinates are normalized, this way one CT normalized image corresponds to one MRI, and both images have the same slice thickness. The first slice correspondence between MR/CT is manually determined, and the subsequent correspondence is automatic. If necessary manual correction can be done.

The lung vessels are segmented from the MR-MIT image by selecting the pixels with intensity higher than a threshold (see Fig. 2). CT image resolution is adjusted to MRI resolution by applying a Gaussian filter in which the parameters are determined by manipulating MR/CT frequency components. The lung contour is determined in the CT and MR images, then pixel intensity is adjusted just internally to the lung. The CT image is binarized, then a labeling algorithm is applied to determine the left and right lungs, and a morphological operator is used to smooth the lung boundary (see Fig. 4.(a)). The MR-MIT image is binarized using a threshold. The heart

[1]MR imaging has a balance between speed and quality.

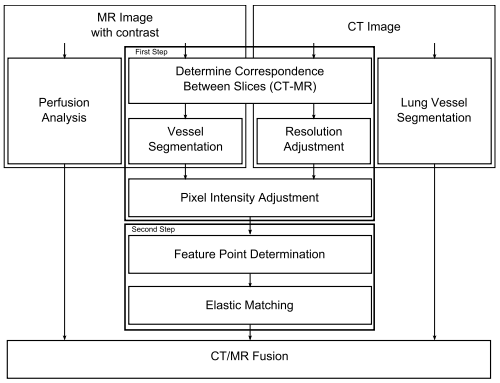

Fig. 3. Proposed MR/CT fusion algorithm shown in the internal rectangles (first and second steps).

(a) (b) (c)

Fig. 4. (a) Lung segmented from CT image. (b) Heart segmented from MR–MIT image. (c) Lung segmented from MRI.

can be segmented by assuming that the contrast concentrates at it (see Fig. 4.(b)). One MRI from the temporal sequence is selected, pixels with higher intensity are associated with water. After a first binarization, the heart that was previously obtained from the MR-MIT image is removed. The lung correct regions are manually selected. Finally, morphological operators are applied to smooth the lung boundary (Fig. 4.(c) shows the final result).

The pixel intensity is adjusted just internally to the previously determined lung masks. Each modality might have different number of bits, the intensity interval from both images is converted to 8 bits. Fig. 5.(a) and (b), respectively, show one MR and CT images with their corresponding masks applied. Fig. 5.(c) shows the result after applying pixel intensity histogram normalization to the CT image. All the processing executed until now, have the objective to approximate the lung features from MR and CT images. One might compare Figs. 5.(a) and (c).

B. Feature Point Determination and Elastic Matching

The Harris corner detector [7] is used, internally to the lung mask, to determine robust features in the MRIs.

(a) (b) (c)

Fig. 5. (a) MRI with the mask determined in Fig. 4.(c). (b) CT image with the mask determined in Fig. 4.(a) applied. (c) Result after pixel intensity histogram normalization is applied to the CT image.

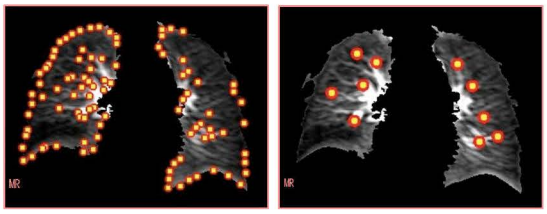

(a) (b)

Fig. 6. (a) Lung features determined using the Harris corner detector [7]. (b) The 5 most confident features picked.

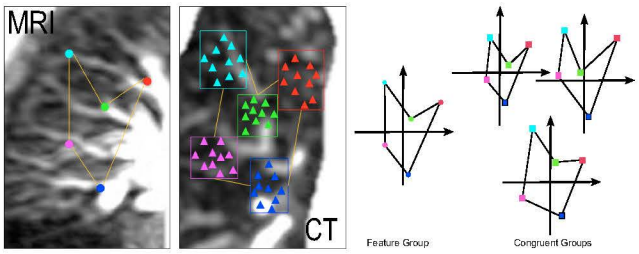

(a) (b) (c)

Fig. 7. (a) The 5 feature points in the MRI. (b) The 5 groups of feature points determined in the CT image, each one with 10 elements. (c) The feature points from the CT image that define a congruent group are analyzed for possible correspondence.

Fig. 6.(a) shows the determined lung features. For each determined feature, a voting procedure is executed to determine the most confident feature considering a square with side r_1, where r_1 is around 30% of the determined lung height. The 5 most confident features Q_i^{MR}, $1 \leq i = 1, \cdots, 5$, are picked. Fig. 6.(b) shows the picked 5 most confident lung features. The square side is reduced if no 5 most confident features can be picked.

For each of the 5 features Q_i^{MR}, $i = 1, \cdots, 5$, a template matching algorithm is used to determine up to 10 possible correspondences Q_{ij}^{CT}, $i = 1, \cdots, 5$, $j = 1, \cdots, 10$, in the CT images. The 5 MR features define a topological configuration as shown in Fig. 7.(a). The 10 possible correspondences in the CT image define 5 groups of features (see Fig. 7.(b)). One feature point from each CT group is combined to define a congruent group $\{Q_{1k_1}, Q_{1k_2}, Q_{1k_3}, Q_{1k_4}, Q_{1k_5}\}$, where $k_l = 1, \cdots, 10$, $l = 1, \cdots, 5$. A valid correspondent group must have the same topology as the original MR feature group, in this case it is said that both groups are congruent (see Fig. 7.(c)). This way the feature group that minimizes

$$B = d_{\max} \times \sum_{i=1}^{5} [1 - R_{CC}(Q_i^{MR}, Q_{ik_i}^{CT})] \qquad (1)$$

is selected, where $R_{CC}(Q_i^{MR}, Q_{ik_i}^{CT})$ is the correlation between both feature points and $\{Q_{ik_i}^{CT}\}$ is a correspondent group in the CT image. $d_{\max}$ is the maximum weight distance that is calculated as

$$d_{\max} = \max_i \{P_i^{MR} - P_i^{CT}\}$$

$$P_i^{MR} = d(Q_i^{MR}, G^{MR}) / \sum_{k=1}^{5} d(Q_k^{MR}, G^{MR})$$

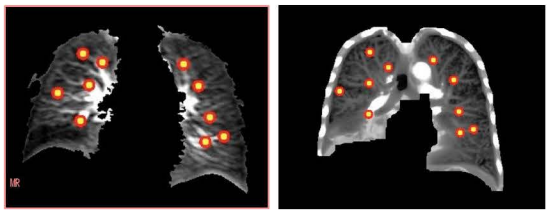

(a) (b)

Fig. 8. (a) The 5 MRI features. (b) The 5 CT image mapped features.

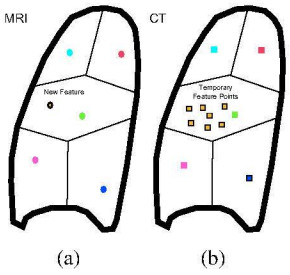

(a) (b)

Fig. 9. (a) MRI with the Voronoi diagram and a new feature candidate. (b) CT image with the Voronoi diagram and possible correspondent features.

$$P_i^{CT} = d(Q_{ij_i}^{CT}, G^{CT}) / \sum_{k=1}^{5} d(Q_{kj_k}^{CT}, G^{CT})$$

where G^{MR} and G^{CT} are the center points for the MR and CT feature groups and $d(.,.)$ is the Euclidian distance between two points.

Figure 8 shows a correspondence. A Voronoi diagram is created using the 5 feature points. This way, it is possible to define a Voronoi region correspondence between MR and CT images. For all remaining MR feature points, correspondent CT feature points are searched in the correspondent internally to the correspondent Voronoi region using expression (1) (see Fig. 9).

Finally, the determined feature mapping are used as input to the metamorphosis algorithm proposed by Beier and Neely [8]. Using the metamorphosis, new CT feature candidates can be mapped back to the MRI.

V. Results

The sequences of MRIs [2] used in the experiment were obtained from a patient with lung cancer lying supine inside a 1.5 T Intera (Philips Medical Systems). A total of 12 slices defining a 3D MR volume was taken in 16 distinct time instants, slice thickness of 12 mm, matrix size = 256×256 pixels, pixel size of 1.68×1.68 mm^2 and 12 bits per pixel. The CT image has 296 images with 512×512 pixels, slice thickness of 1 mm and pixel size of 0.723×0.723 mm^2.

Figure 10 shows some registration results from the proposed algorithm. Fig. 10.(a) shows the MRI with the original 5 feature points. Fig. 10.(b) shows the 5 registered CT feature points. Fig. 10.(c) shows the all the original MR features and some additional features inversely mapped from the CT

[2]The protocol was approved by the hospital medical-ethics committee of Kanagawa Cardiovascular Respiratory Center, and informed consent was obtained from the patient.

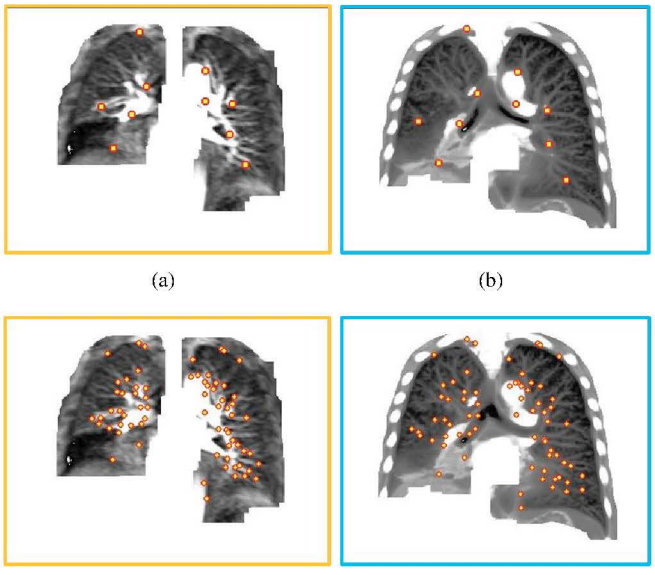

(a) (b)

(c) (d)

Fig. 10. (a) The 5 MRI features. (b) The 5 CT image mapped features. (c) All determined features in the MRI. (d) The mapped features in the CT image.

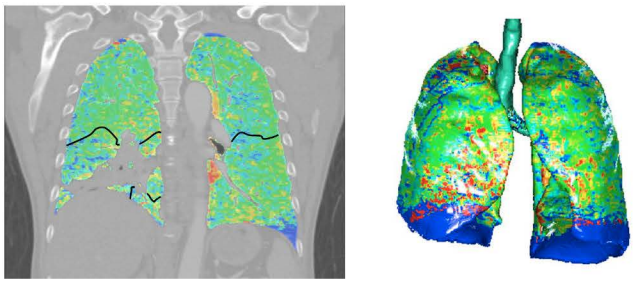

(a) (b)

Fig. 11. (a) Perfusion analysis result shown in a CT image where the lobes where automatically classified (the black line shows the interlobe surface). (b) Semi transparent lung with perfusion analysis result.

image. Fig. 10.(d) shows a CT image with features registered from the MRI and additional features determined in the CT image.

The point correspondence was visually verified, and the proposed algorithm showed to be averagely 80% correct. The temporal MRIs with contrast was used as input for a blood perfusion analysis and the result was mapped in the segmented lung vessel tree and CT images. Fig. 11.(a) shows the perfusion analysis result registered with a CT image. Fig. 11.(b) show a semi transparent lung with the registered perfusion analysis result. Fig. 12.(a) shows transparent lungs with the lung vessel tree with registered perfusion analysis result. Fig. 12.(b) shows some lung lobes with the lung vessel tree with registered perfusion analysis result.

VI. Conclusions and Future Works

A multimodality MR/CT registration algorithm was proposed. Initially, lung CT and MR images are normalized, feature points are determined and an elastic matching is performed. The obtained mapping registration was used to

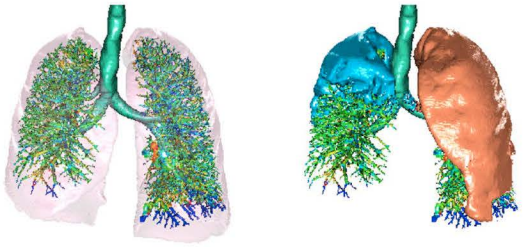

(a) (b)

Fig. 12. (a) Perfusion result shown with transparent lungs. (b) Perfusion result shown with two lobes.

combine MR perfusion analysis result with segmented lung vessel tree. The proposed method can be improved if the segmented lung vessel tree is simultaneously used with the proposed registration algorithm. Additionally, the segmented lobes from the CT image can be mapped into the 3D MRI and the perfusion at each lobe can be determined. As future work, numerical and clinical evaluations of such algorithm are under research.

VII. Acknowledgements

We are indebted to all patients and all the residents working in our units during the study period for their dedication and collaboration in providing care to the patients that participated in this research.

References

[1] W. R. Crum, L. D. Griffin, D. L. G. Hill, and D. J. Hawkes, "Zen and the art of medical image registration: correspondence, homology, and quality", *NeuroImage*, vol. 20, pp. 1425–1437, 2003.

[2] T. Gotoh, Y. Hosoda, T. Yanagita, S. Kagei, T. Iwasawa, T. Inoue, and M. S. G. Tsuzuki, "Motion complexity analysis with automated lung field tracking in MRI temporal sequences", in *Proc 18th IFAC World Congress*, 2011, pp. 5001-5006.

[3] K. Murphy, B. van Ginneken, J. M. Reinhardt, S. Kabus, K. Ding, X. Deng, K. Cao, K. Du, G. E. Christensen, V. Garcia, T. Vercauteren, N. Ayache, O. Commowick, G. Malandain, B. Glocker, N. Paragios, N. Navab, V. Gorbunova, J. Sporring, M. de Bruijne, X. Han, M. P. Heinrich, J. A. Schnabel, M. Jenkinson, C. Lorenz, M. Modat, J. R. McClelland, S. Ourselin, S. E. A. Muenzing, M. A. Viergever, D. de Nigris, D. L. Collins, T. Arbel, M. Peroni, R. Li, G. C. Sharp, A. Schmidt-Richberg, J. Ehrhardt, R. Werner, D. Smeets, D. Loeckx, G. Song, N. Tustison, B. Avants, J. C. Gee, M. Staring, S. Klein, B. C. Stoel, M. Urschler, M. Werlberger, J. Vandemeulebroucke, S. Rit, D. Sarrut, J. P. W. Pluim, "Evaluation of registration methods on thoracic CT: The EMPIRE10 challenge", *IEEE Trans. Med. Imaging*, vol. 30, pp. 1901-1920, 2011.

[4] X. Wang, C. Fang, Y. Xia, and D. Feng, "Airway segmentation for low-contrast CT images from combined PET/CT scanners based on airway modelling and seed prediction", *Biomed. Signal Proces. Control*, vol. 6, pp. 48-56, 2011.

[5] T. Schlathoelter, C. Lorenz, I. C. Carlsen, S. Renisch, and T. Deschamps, "Simultaneous segmentation and tree reconstruction of the airways for virtual bronchoscopy", in *Proc. SPIE Conf. Medical Imaging: Image Processing*, 2002, pp. 103-113.

[6] Y. Iwao, T. Gotoh, S. Kagei, T. Iwasawa, and M. S. G. Tsuzuki, "Integrated lung field segmentation of injured regions and anatomical structures from chest CT images", in *Proc. 8th IFAC Symp. Biological and Medical Systems*, Budapeste, Hungary, 2012, pp. 85-90.

[7] C. Harris and M. Stephens, "A combined corner and edge detector", in *Proc. 4th Alvey Vision Conf.*, 1988, pp. 147-151.

[8] T. Beier and S. Neely, "Feature-based image metamorphosis", in *Proc. 19th Annu. Conf. Computer Graphics and Interactive Techniques*, SIGGRAPH 92, New York, USA, 1992, pp. 35-42.